MNRAS 000, 1–11 (2019) Preprint 10 December 2019 Compiled using MNRAS LATEX style file v3.0

Magnetic activity and evolution of the four Hyades K giants

K.-P. Schröder[1,3⋆], M. Mittag[2], D. Jack[1,2], A. Rodríguez Jiménez[1], J.H.M.M. Schmitt[2]

[1] *Depto. Astronomia, Universidad de Guanajuato, A.P. 144, Guanajuato, GTO, C.P. 36000, Mexico*
[2] *Hamburger Sternwarte, Universität Hamburg, Gojenbergsweg 112, D-21029 Hamburg, Germany*
[3] *Sterrewacht Leiden, Nils Bohrweg 2, NL-2333CA Leiden, Netherlands*

10 December 2019

ABSTRACT

We determine the exact physical parameters of the four Hyades cluster K giants, using their parallaxes and atmospheric modeling of our red-channel TIGRE high-resolution spectra. Performing a comparison with well-tested evolutionary tracks, we derive exact masses and evolutionary stages. At an age of 588 (±60) Myrs and with a metallicity of Z=0.03 (consistent with the spectroscopic abundances), we find HD 27371 and HD 28307, the two less bright K giants, at the onset of central helium-burning, entering their blue loops with a mass of 2.62 $M_{\odot}$, while the slightly brighter stars HD 28305 and HD 27697 are already exiting their blue loop. Their more advanced evolution suggests a higher mass of 2.75 $M_{\odot}$.

Notably, this pairing coincides with the different activity levels, which we find for these four stars from chromospheric activity monitoring with TIGRE and archival Mount Wilson data as well as from ROSAT coronal detections: The two less evolved K giants are the far more active pair, and we confidently confirm their rotation with periods of about 142 days. This work therefore provides some first, direct evidence of magnetic braking during the 130 Myrs lasting phase of central helium-burning, similar to what has long been known to occur to cool main-sequence stars.

Key words: Stars: giants – Stars: chromospheres – Stars: activity

1 INTRODUCTION

After the discovery of chromospheric Ca II H&K line emission as a possible activity indicator by Eberhard & Schwarzschild (1913), it was mainly Olin C. Wilson and his collaborators at the Mount Wilson Observatory, who carried out much of the early work on chromospheric activity. The Ca II H&K line emission was observed for all kinds of stars (Duncan et al. 1991) across the HR diagramme (HRD), and a spectroscopic activity monitoring programme of solar-like stars resulted in the discovery of stellar activity cycles similar to the solar 11 year Schwabe cycle (Baliunas et al. 1995).

Since the early 1960ies, this research benefited from the introduction of an easily measurable quantity, the so-called S-index, and a specific four-channel narrow-band spectrophotometer designed by O.C. Wilson for making instantaneous S-index measurements (see Vaughan et al. (1978) with more details given below). As a consequence, the magnetic activity observed for the Sun could finally be juxtaposed to the activity observed for stars and thus the Sun could be put in its proper stellar perspective.

O.C. Wilson's historic work on chromospheric Ca II H&K emission of giant stars is fundamental (e.g. Wilson & Bappu (1957)), since a number of brighter giants had been included in his chromospheric activity monitoring programme, which started in the 1960ies. However, since most of the cooler giants do not show coronal X-ray emission (Linsky & Haisch 1979), doubt was cast on their activity, until it became understood (see, e.g, Ayres et al. (1997)), that magnetic activity does continue into the most evolved stages of stellar evolution. The more recent findings of direct evidence of magnetic fields in giant stellar photospheres leave no doubt on this issue (Hubrig et al. (1994), Konstantinova-Antova et al. (2013)).

Unfortunately, this line of research of the Wilson group was never published in a refereed publication. In fact, cool giants are a mixed group of stars with very different masses and different evolutionary states, in addition, there are observational and other complications (see Schröder et al. (2018) for a recent discussion). Most K giants, however, are simpler. The large majority is in the relatively stable phase

⋆ email: kps@astro.ugto.mx

of central helium burning, and as such are intermediate to giants on the red giant branch (RGB) and asymptotic giant branch (AGB).

As a consequence, the Hyades K giants are of a particular interest for an understanding of how magnetic activity evolves with the star. Ever since Skumanich (1972) demonstrated a relation between increasing age and decreasing activity of a star, the importance of magnetic braking of stellar rotation has been recognized. In the case of main sequence stars (see, e.g., Schröder et al. (2013) and references given therein), in particular from measurements of the chromospheric Ca II H&K emission there is convincing observational evidence for the action of magnetic braking; in that work we also find that activity on the main sequence appears to decline with the age *relative* to the star's main sequence life-time, since both, magnetic breaking and evolution timescales depend on the stellar mass in a similar way.

Also, from X-ray detections across the HRD we know that recent Hertzsprung gap crossers are very active again, and that the K clump giants of the solar neighbourhood still have moderate coronal emission - their range of X-ray surface fluxes is comparable to that of the Sun (Hünsch et al. 1996a). With magnetic activity also found on the AGB (see Duncan et al. 1991, Schröder et al. 2018), the main question here is, whether we observe a down- or an upturn of activity during central helium burning. Such empirical evidence is crucial to understand the evolution of the internal angular momentum and how it shapes dynamo action as well as the interplay with magnetic braking.

Therefore, the four bright and nearby Hyades K giants are an obvious starting point for such research. Already more than 35 years ago, Baliunas et al. (1983) combined observations of chromospheric emission by means of the S-index and UV emission lines observed by IUE as well as coronal X-ray detections from the *Einstein Observatory*, to come to ask the important question: Why and how can these four giants of the same age and almost the same mass and structure be so different in their activity levels?

Based on his chromospheric activity monitoring measurements, this question occurred to O.C. Wilson already in 1972 (private communication through D. Reimers to one of us (KPS)). When our robotic 1.2 m telescope TIGRE with its high-resolution spectrograph HEROS started its operations at Guanajuato in 2014 (Schmitt et al. 2014), all four Hyades K giants were included in TIGRE's chromospheric activity monitoring programme.

Consequently, this paper looks at the exact evolution states of these four K giants (section 2) and at their activity (section 3), by briefly reviewing the X-ray observations and analyzing in depth the chromospheric activity monitoring of the Mount Wilson group and by ourselves with TIGRE.

2 EVOLUTIONARY STATES: A SMALL BUT CRUCIAL DIFFERENCE

Before turning to a discussion of the activity properties of the Hyades giants, we begin with an assessment of the individual evolutionary states of these objects. The Hyades cluster is not very rich in stars; for example, in the recent study of Hyades membership based on Gaia parallaxes Lodieu et al. (2019) find 710 members within a distance of 30 pc from the cluster center, with 85 members being located in the actual cluster core, and the same authors identify 8 brown dwarfs and verify their Hyades membership. Yet, the Hyades also contain a sufficient number of evolved stars. Again based on Gaia parallaxes, Salaris & Bedin (2018) find at least 8 white dwarfs as Hyades cluster members, which as the more massive stars have already passed the red giant stage.

The four prominent K-type Hyades giants (ϵ Tau, δ Tau, γ Tau, θ^1 Tau) have been known for a long time. This surprisingly large number is based on the speed of stellar evolution: The stars in question have masses of about 2.7 $M_\odot$ (see our discussion below), and their central helium-burning lifetime of about 130 million years accounts for as much as 20% of the total stellar lifetime. In the case of the Sun, for example, central Helium-burning accounts only for 1% of its lifetime, and therefore such low-mass K giants are found in much smaller fractions (say one per hundred main sequence stars). Consequently, the number of K clump giants can be a lot smaller in clusters, which differ from the Hyades in turn-off mass and hence age. This little detail makes the Hyades K giants an excellent test bed for a study of how stellar evolution evolves during central helium burning.

2.1 Assessment of the exact physical parameters

The two most important stellar parameters, distinguishing the Hyades K giants from one another, are luminosity L and effective temperature $T_{\rm eff}$. Since the individual parallaxes of the Hyades giants are now known, the main remaining uncertainty comes from the values adopted for the bolometric correction and the solar bolometric magnitude. In Table 1 we list the parallaxes, luminosities and all other stellar quantities relevant for our study.

For the luminosities as given in Table 1, we use BC = 0.50 for all four K giants, since their colours are very similar, and $M_{\rm Bol\odot}$= 4.74, consistent with long-standing calibrations like the one given by Schmidt-Kaler (1982). At least this choice does not affect the relative differences between these giants, which matter most for this study. Somewhat smaller bolometric corrections favoured by more recent compilations, which suggest a BC around 0.4 for the Hyades K giants (e.g. Flower (1996)), would result in slightly smaller masses, i.e., less by up to 2.5% or 0.07 $M_\odot$ for all four giants, and an age up to 10% (60 Myrs) larger than the values given below, but there would be no change in the relative differences.

To derive effective temperatures from our high s/n (up to 200) R = 21000 TIGRE/HEROS spectra, we use the spectra analysis tool iSpec (Blanco-Cuaresma et al. 2014), working on the orange-red part of the spectrum, from which we excluded small spectral regions with line blends, to avoid confusion. Regions contaminated with telluric lines have also been excluded from the analysis, which is based on a comparison with a library of synthetic spectra (ATLAS9 of Kurucz (1993)) and the line list of the Vienna Atomic Line Data Base (VALD, Piskunov et al. (1995)), employing the SPECTRUM code. As a reference to the solar abundances, we use Asplund et al. (2009).

To obtain the most reliable results, we follow the recommendation of Blanco-Cuaresma et al. (2019) to keep as many parameters fixed as possible, which reduces the errors

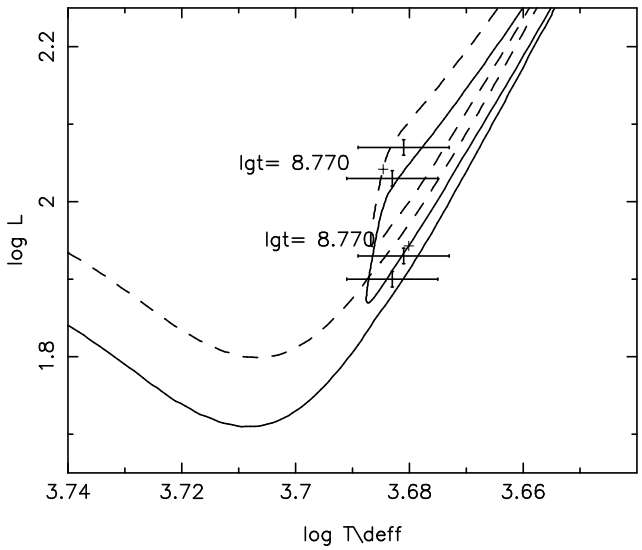

Figure 1. Evolution models for a metallicity of Z=0.03 (close to [Fe/H]=+0.2) and with stellar masses of 2.62 (solid line) and 2.75 $M_\odot$ (- -) fit all four Hyades K giants at their HRD positions for an age of 588 Myrs: HD 27371 and HD 28307 at the onset of central helium-burning, which lasts 130 Myrs and forms the blue loop, while the slightly brighter pair of HD 28305 and HD 27697 is already exiting the blue loop.

of the parameters to be derived. In our case, we derive the mass from matching evolution tracks, and with a preliminary value for $T_{\rm eff}$ we then calculate $\log g$, which we find close to 2.5 in all four stars, and so use it as a fixed value in the automatic iSpec analysis. We estimate the remaining uncertainty in $T_{\rm eff}$ to be under 100 K or 0.008 dex (see error bars in Fig. 1). The abundances as obtained by this method by us lie in the range given by a vast literature (see, e.g., Perryman et al. (1998), Ramya et al. (2019) and citations therein), and fall around [Fe/H]=0.22.

2.2 Derivation of the exact states of evolution

The HRD positions resulting above need to be compared to suitable evolution models, which we computed with the Cambridge (UK) Eggleton code in its updated version. Significant improvements were made with respect to opacities and equation of state as described by Pols et al. (1997) and Pols et al. (1998); in these papers a detailed description of our procedures is given, here we provide only a summary. While the code is using a classical mixing-length-theory approach to convection, it differs from others in solving an additional equation to optimize the spread of its height points and concentrate them in layers of steep gradients like burning shells. This concept makes the code economic with respect to CPU time and robust, as it works well with only 200 height points.

For central hydrogen burning models for main sequence stars, like all evolution codes, the luminosity at any given mass depends on the used equation of state and on the choice of helium abundance. For cool stars with large convective envelopes, their radii and effective temperatures depend on the parameterization of the convective length scale in terms of the pressure scaleheight, $l_c = \alpha H_P$. As described in the first of the above papers, we use a best-choice of $\alpha = 2.0$, where $\alpha = 2.0$. In addition, for stars with masses larger than about 1.5 $M_\odot$, the prescription of convective core overshoot, which empirically and indiscriminately includes all kind of extra mixing beyond the Schwarzschildt boundary, plays an important role from the later central hydrogen burning onwards.

The second of the above papers demonstrates an excellent agreement of these models of the code (as used here) with eclipsing binaries of well-known physical parameters. These models also agree very well with those of the classical Geneva code of Meynet et al. (1993). Apparently, slightly different choices of the helium abundance Y (adopting a slightly different $\Delta Y/\Delta Z$) compensated for small differences in the equation of state. Our models use Y = 0.28 for a nearly solar metalicity of Z=0.02, and Y=0.30 for Z=0.03 (as then used here for modeling the moderately iron-rich Hyades giants, and for the models shown in Fig. 1). Later, based on another type of evolutionary code, models were published by Pietrinferni et al. (2004) and Pietrinferni et al. (2006), which also agree very well with the resulting physical parameters of our models.

The amount of core overshooting prescribed on the medium-mass, central hydrogen burning of a stellar model has an ever increasing effect on the mass of the resulting helium core in the evolving star. Consequently, the brightness of the resulting red giant provides – especially during the central helium burning (blue loop) phase – a very sensitive test of this issue, whenever the respective stellar mass is well known. This idea was carefully employed by Schröder et al. (1997), using giants in eclipsing (ζ Aur type) binaries with masses, luminosities, radii and effective temperatures well known from observations. Based on this approach, the resulting overshoot parameterization (used here with the very same code) empirically accounts for all extra mixing beyond the convective, hydrogen-burning core (apart from genuine overshooting, this can be, e.g. the average meridional mixing by rotation). For the masses of the Hyades K giants (see below), our models employ a nominal overshoot length of $l_{ov} = 0.24 H_P$, which is slowly rising to $0.3 H_P$ for larger masses, see Fig. 10 in Schröder et al. (1997). For further technical detail on the evolution code and its parameterization used here, we like to refer the reader again to Pols et al. (1997) and Pols et al. (1998).

Assuming that all four Hyades giants have the same age, they then must have slightly different masses to show somewhat different advances of their stellar evolution. For this assessment, we compared a variety of evolutionary tracks to the HRD positions obtained above. Where these tracks, to within the observational uncertainties, can be met by different stages of evolution, we gave preference to the slowest phase (such as the blue loop, which marks the stable central helium burning), since the probability for finding a star at point in the HRD is simply larger. The same argument makes a fast phase, e.g., the very swift ascent on the RGB or the climbing of the AGB, a per se unlikely choice. The other strongly discriminating condition is, as pointed out above, that all final models must not only match the observed HRD positions, but also have the same age.

In this fashion and using the physical quantities given in Table 1, we find masses of (i) 2.62 $M_\odot$ for the less bright pair, which has just come down the RGB to start central helium

Table 1. Astrophysical quantities and activity indicators of the four Hyades K giants. Parallax values are courtesy to GAIA DR2, obtained from VizieR of the Strasbourg astronomical data centre.

star	π [mas]	$\log L$ $[L_\odot]$	$\log T_{\rm eff}$ [K]	M $[M_\odot]$	R $[R_\odot]$	$< S >$	L_X $[10^{29} ergs^{-1}]$	F_x $[10^4 erg\ cm^{-2} s^{-1}]$
HD 28305/ϵ Tau	20.31	2.07	3.681	2.75	15.8	0.129	0.15	0.10
HD 27697/δ Tau	19.06	2.03	3.683	2.75	14.9	0.133	0.54	0.40
HD 27371/γ Tau	22.62	1.93	3.681	2.62	13.4	0.178	11.60	10.45
HD 28307/θ^1 Tau	21.42	1.90	3.683	2.62	12.8	0.166	18.43	18.16

burning and turned off the main sequence only 10 Myrs ago, and (ii) of 2.75 $M_\odot$ for the brighter pair, which is about to finish central helium burning, which according to our models lasts 130 Myrs. This is long enough to tell us about evolutionary changes in the level of the K giant activity, as we will demonstrate in the next section. We reemphasize our assumption that all four giants have the same age, which implies that we attribute their evolutionary differences, i.e., start and end of central helium burning, solely to the mass difference of 0.13 $M_\odot$, which causes the two more luminous and more massive giants to be more evolved than the less massive giant pair.

Since all other possible matches with evolutionary tracks would set either the one or the other pair of giants outside the blue-loop segment – that is: not one, but always two stars have a less likely, fast evolutionary state – the solution presented here in Fig. 1 is significantly more probable than any other formally possible solution, since for the four giants taken together, the probabilities of matching any individual star multiply with each other. In consequence, this approach of ruling out other matching choices involving faster episodes in evolution, is much stronger for a set of stars like the four K giants studied here than it is for a single star.

The Hyades cluster age of our models shown in Fig. 1, is 588 Myrs, in good agreement with Gossage et al. (2018) (in particular with their model for a rotation of $\Omega/\Omega_c = 0.6$) and references given therein. A long-standing literature age of the Hyades is 625 Myrs (Perryman et al. (1998)). As mentioned above, the uncertainty in luminosity of about 10% due to a possibly lower BC of 0.4 would give us alternative models with slightly smaller masses and, consequently, of an age of up to 648 Myrs. Hence, the age agreement lies reasonably well within this and other uncertainties. Furthermore, we should note that our models shown in Fig. 1 suggest a mass of 2.60 $M_\odot$ at the turn-off point.

3 ACTIVITY OF THE HYADES K GIANTS

3.1 Coronal activity: X-ray emission

In the X-ray range Stern et al. (1981), using the *Einstein Observatory*, obtained the first detections of X-ray emission from the Hyades giants and measured X-ray luminosities of $10^{29.4}$ erg/s, $10^{28.9}$ erg/s, and $10^{30.0}$ erg/s for the stars γ Tau, δ Tau, and θ^1 Tau, respectively, while the star ϵ Tau was outside the field of view and thus remained unobserved by the *Einstein Observatory*.

Naturally, the Hyades region was scanned in the context of the ROSAT all-sky survey (RASS) and in their RASS study of the Hyades region Stern et al. (1995) report the X-ray detections of all four Hyades giants. Using the most recent RASS catalog by Boller et al. (2016) we identify the RASS sources 2RXS J041947.5+153739 with γ Tau, 2RXS J042252.4+173148 with δ Tau, 2RXS J042836.6+191036 with ϵ Tau and 2RXS J042834.7+155721 with θ^1 Tau, respectively, which were observed with count rates of 0.44 ± 0.04 cts/s, 0.03 ± 0.01 cts/s, 0.02 ± 0.01 cts/s, and 0.81 ± 0.04 cts/s respectively.

Hence, the dichotomy between γ Tau and θ^1 Tau (HD 27371 and HD 28307) on the one hand, and δ Tau and ϵ Tau (HD 27697 and HD 28305) on the other hand is immediately apparent in the observed RASS rates, with clear detections for the former (active) pair, and almost marginal detections for the latter pair of Hyades K giants. However, later pointed ROSAT observations of δ Tau (in ROSAT sequence RP200442) with a count rate of 0.0250 ± 0.0012 cts/s and of ϵ Tau (in ROSAT sequence RP200576) with a count rate of 0.0101 ± 0.0007 cts/s provided clear confirmations of all RASS detections.

Using these count rates we can compute X-ray fluxes, X-ray luminosities and X-ray surface fluxes, using the count-flux-conversion by Schmitt et al. (1995), and thus arrive at the numbers quoted in Table 1. It is important to keep in mind that detailed spectral information is not available from the ROSAT data, the flux conversion is therefore fraught with considerable uncertainty, which we estimate to be on the order of 50 %. And we need to keep in mind that, while active stars are variable, these X-ray detections are based on only a small number of visits.

Nevertheless, a bifurcation is clearly seen into two active and two inactive K giants, very much like (as shown below) is the result of chromospheric activity monitoring, even though X-ray data do not yield any significant ranking order within each of these two pairs.

3.2 Chromospheric activity

3.2.1 Ca II H&K emission: the S-index

For this paper we use the results of spectral monitoring with our TIGRE facility (Schmitt et al. 2014), as well as the S-index time series obtained in the framework of the Mount Wilson H&K project. The TIGRE facility is a fully robotic telescope with a 1.2 m aperture, located at the La Luz Observatory near Guanajuato, Mexico. Its only instrument is the two channel fiber-fed Échelle spectrograph HEROS with the wavelength range from 3800 Å to 8800 Å with a 100 Å gap at 5800 Å and a spectral resolution of, according to

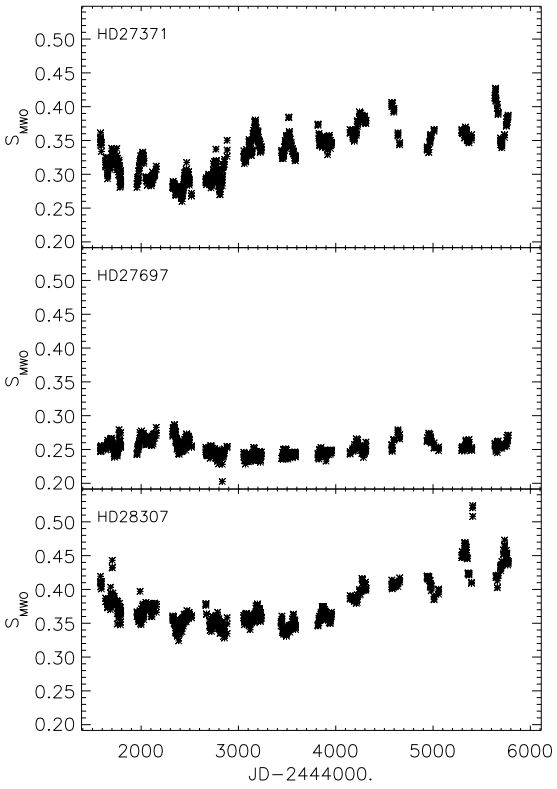

Figure 2. Mt. Wilson S-index times series of the Hyades giants HD 27371 (top panel), HD 27697 (medium panel) and HD 28307 (bottom panel). The zero point corresponds to Jan 30, 1982 and data have been obtained in twelve consecutive observing seasons; see text for details.

our recent performance measurements, R≈21000; a detailed description of TIGRE is given by Schmitt et al. (2014).

In addition we use data obtained by the Mount Wilson H&K Project, which have been made available to the public and can be downloaded from ftp://solis.nso.edu/MountWilson_HK/; a detailed description of the data is also provided at this web site. The available data specifically include the star identification; the calibrated S index, which we use in this paper as the basis for our analysis; a code indicating with which instrument the data was taken; as well as the date of the observation and other material.

It is important to keep in mind that the hardware used by the TIGRE and Mount Wilson H&K Projects is fundamentally different. While TIGRE is using an Échelle spectrograph, which covers, in particular, the whole region of the Ca II H and K lines, the Mount Wilson H&K Project used a four channel photometer, where the four channels were realized by an exit multi-slit configuration on a rotating disk, which allowed subsequent measurements of the output channels with a frequency of about 30 Hz; a detailed description of this hardware is provided by Vaughan et al. (1978). In this fashion measurements of the so-called R-band (between 3991.067 Å and 4011.067 Å) and V-band (between 3891.067 Å and 3911.069 Å) were obtained, while the actual H and K fluxes were measured in two narrow bands with a FWHM of 1.09 Å centered on the H and K lines respectively. The S-index was then calculated from the relation

$$S = \alpha \frac{N_H + N_K}{N_R + N_V}, \quad (1)$$

where the quantity N_i denote the recorded number of counts in the band i, and α is a correction factor, which is used to make measurements with different hardware compatible with each other.

This definition and simultaneous measurement procedure of the S-index provides an activity record which is largely independent of atmospheric conditions, since changes in atmospheric throughput or transmission cancel out by its definition as a ratio between two measurements. Since it also comes with a list of over 40 calibration stars, it can be used independently of the instrumentation for comparison with measurements from over six decades ago to look for long-term variability of chromospheric activity of any star already observed back then at Mt. Wilson (see Schröder et al. (2018) for a more detailed discussion). On the other hand, a lot of the spectral information is lost in the S-index construction, which is of course retained in the TIGRE spectroscopic data, yet it is very useful to compute an S-index from the TIGRE data with a procedure described in detail by Mittag et al. (2015).

In our TIGRE spectra, we can inspect the emission line profiles to check for their width, which is wider than the emission of main sequence stars, according to the Wilson-Bappu effect (Wilson & Bappu 1957). The TIGRE S-index is based on the well-calibrated 1 Å bandpath, and luminous giant Ca II H&K emission exceeds that width. For all Hyades giants, however, we find that always about 95% of their chromospheric emission is included. Consequently, its variations are well proportional to the variable surface flux caused by chromospheric heating of the K giants and have no other source (i.e., we find no noticeable variations in wavelength relative to the photospheric profile).

3.2.2 Mount Wilson observations

An important aspect for studying long-term variability of stellar magnetic activity is that S-index measures are available from over six decades ago (see Schröder et al. (2018) for a more detailed discussion), and the Mount Wilson data base includes time series measurements of the Hyades K giants HD 28307, HD 27371 and HD 27697. Nevertheless, only the data for HD 28307 seem to have been published (see Fig. 1 in Choi et al. (1995)). For HD 28305 only a single S-index measurement exists, but no time series.

As pointed out and described by Choi et al. (1995), those measurements were taken with a 2 Å wide bandpass dedicated to giants, to mitigate the above-mentioned Wilson-Bappu effect, and are therefore not directly comparable to measurements taken with the "standard" narrow bandpass, as used by TIGRE S-measurements and all earlier Mount Wilson observations.

In Fig. 2 we show the Mount Wilson S-index data recorded in the time between 1984 and 1992; note that the data for HD 28307 have already been shown by Choi et al. (1995). All data sets appear to suggest the presence of activity-cycles with periods on the order of 15 years, which is the time span of the observations, however, clearly, this

time span of these data is too short to ascertain the existence of cycles with certainty. In addition, the data also show short-term variations, which can be interpreted as rotational modulation and which we will in detail discuss below.

Regardless of such long-term variations, Fig. 2 shows that the S-indices of the two X-ray active giants HD 28307 and HD 27371 are much higher than that of the X-ray weak giant HD 27697, thus the chromospheric emission appears to mirror the X-ray emission well.

3.2.3 TIGRE observations

For reasons of simplicity and calibration, we here now discuss the Hyades K giants activity levels in terms of the standard Mt. Wilson S-index $S_{\rm MWO}$, obtained from TIGRE/HEROS blue channel spectra of the years 2014-2019 in the well-calibrated 1 Å bandpass. Ever since the start of the TIGRE robotic observations in 2014, spectra of the four Hyades giants have been taken on a regular schedule.

Averages and the observed ranges of $S_{\rm MWO}$ for the four Hyades K giants from 6 years of TIGRE monitoring (2014 to 2019) are as given in Table 1 and can be summarized as follows: HD 28305 varies between $S_{\rm MWO} = 0.120$ and 0.150 with an average of $< S >= 0.129$, HD 27697 between 0.120 and 0.155 with $< S > = 0.133$, while the less bright K giants HD 27371 and HD 28307 vary between 0.145 and 0.205 with $< S > = 0.178$, and 0.150 to 0.195, with $< S >= 0.166$, respectively (see also Table 1).

We should note, to put these values into perspective, that a value of 0.12 corresponds to the chromospheric emission of giant stars known to be inactive (see respective Figs. in Duncan et al. (1991) and Fig. 3 in Schröder et al. (2012)), i.e. with only a "basal flux" not related to stellar activity as such.

If we take into account, that stars like the Sun have a somewhat larger "basal flux" level of $S_{\rm MWO}$ than giants, about 0.15 (see Schröder et al. (2012)), then the two active Hyades K giants resemble the activity level of the active Sun. Hence, on average, these are a bit more active than the Sun. Since these giants may be passing different phases of their cycles, an exact ranking between the two of them is premature.

3.3 A clear relation between activity level and evolutionary state

In general, the emerging picture is clear, both from coronal and chromospheric activity: The active pair of giants (γ Tau = HD 27371 and θ^1 Tau = HD 28307) is emitting X-ray surface fluxes about two orders of magnitude larger than does the inactive pair. The latter (ϵ Tau = HD 28305 and δ Tau = HD 27697) hardly reach the minimal coronal surface flux of inactive stars found by Schmitt (1997), $F_{x,min} = o(10^4\,{\rm erg\ cm^{-2}sec^{-1}})$, which resembles F_x of the inactive solar corona, when the star in question is on the left side of the "corona-wind dividing line" in the HRD. According to Linsky & Haisch (1979)), coronal X-ray emission is predominantly found on that left side, while the right (cool) side in the HRD is dominated by cool winds; we note in this context, that the Hyades K giants are very close to this "dividing line".

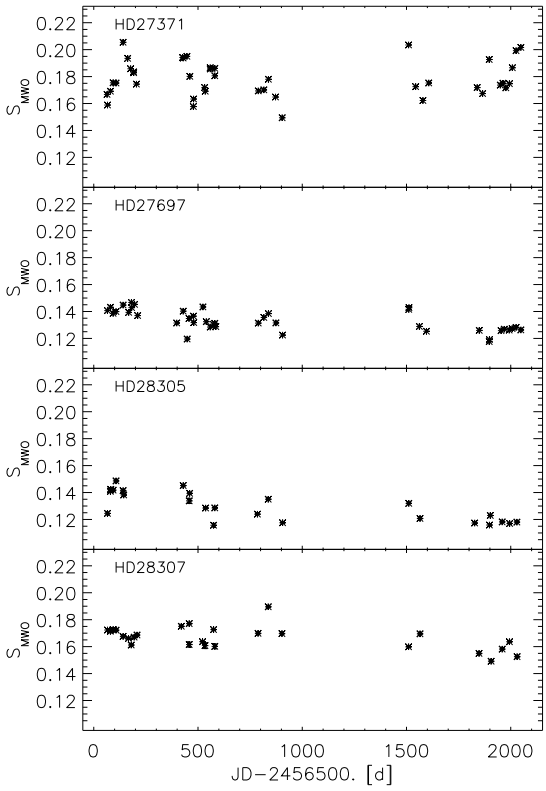

Figure 3. TIGRE chromospheric monitoring of HD 28305 in the years of 2014 to 2019, using the calibrated S-index as defined by the Mt. Wilson work with 1 Å H&K line bandpass.

The same pattern, a split-down into two active and two inactive K giants, is reflected by the chromospheric activity, see the average S-values obtained above for these giants (and see Table 1). It is now instructive to relate the different activity levels of the stars γ Tau (= HD 27371) and θ^1 Tau (= HD 28307) on the one hand, and ϵ Tau (= HD 28305) and δ Tau (= HD 27697) on the other, with their positions on the evolutionary tracks (shown in Fig. 1):

The two active giants θ^1 Tau γ Tau), are only in the beginning of their central helium burning phase, implying that they have just passed the fast RGB, and that their core contraction in the Hertzsprung gap is still very recent. By contrast, the stars ϵ Tau and δ Tau are already in the end stage of their central helium-burning, and have already remained in this stable phase for about 130 Myrs. Their much lower activity thus suggests magnetic braking during this relatively stable period. This process would then be comparable to those in main-sequence stars of lower masses, which have convective envelopes and magnetic activity during their stable central hydrogen-burning phase, i.e. stars with $M < 1.5 M_\odot$, significantly less massive than the Hyades K giants.

3.4 Rotation periods from S-data variability

At first glance, one might expect, just like in the case of main sequence stars, that rotation periods can be obtained

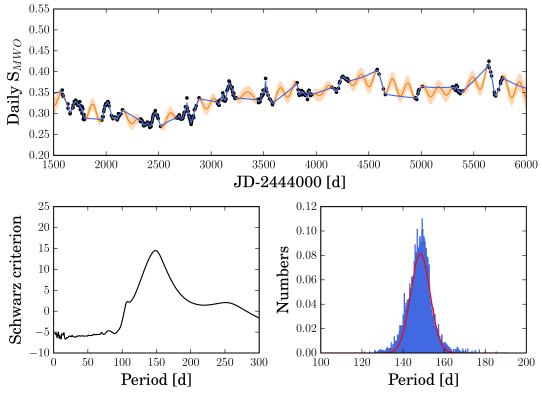

Figure 4. Upper panel: Mount Wilson time series of HD 27371 (blue data points) together with best fit GP (orange curve). Lower panel (left): Schwarz criterion as function of trial period

. Lower panel (right): Results of a Markov chain Monte Carlo simulation of the trial periods; see text for details.

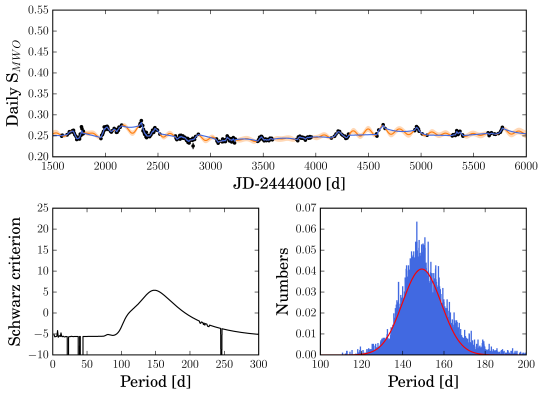

Figure 5. Same as in Fig. 4 with the Mount Wilson data for HD 27697.

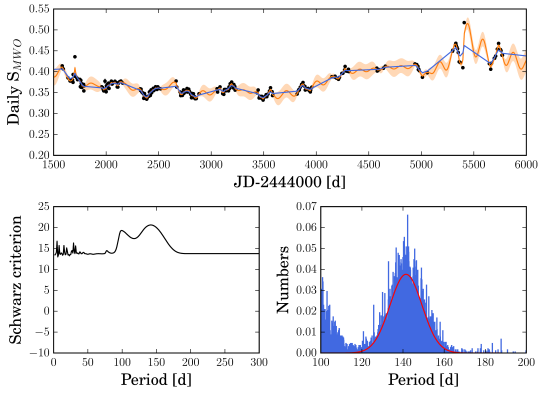

Figure 6. Same as in Fig. 4 with the Mount Wilson data for HD 28307.

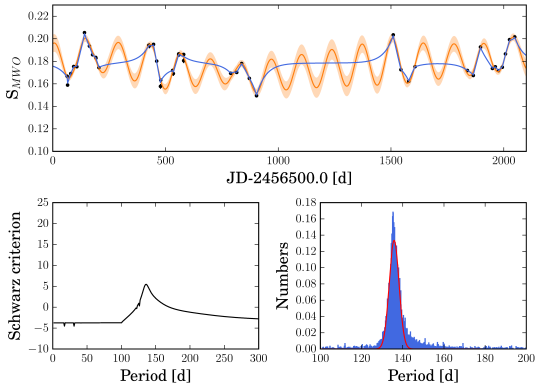

Figure 7. Same as in Fig. 4 with the TIGRE data for HD 27371.

Table 2. Rotational periods

star	$P_{\rm rot}$ [d]	S. criterion
Mount Wilson time series		
HD 27697/δ Tau	148.2±9.4	5.4
HD 27371/γ Tau	148.8±4.7	14.5
HD 28307/θ^1 Tau	141.9±7.8	20.6
TIGRE time series		
HD 27371/γ Tau	136.0±2.4	5.5

from activity monitoring for giant stars as well – utilizing the fact that active regions can be unevenly distributed on the stellar surface.

Nevertheless, the much longer rotation periods of giants make a difference: First, a sufficiently longer monitoring time span is required. While this is a merely technical problem, the limited lifetime of active regions, apparently of the same order of, or shorter than the giant rotation periods, produces a serious interference with the search for the rotational signal. The appearances and disappearances of individual active regions result in peaks in any periodogram, which compete with and confuse the rotational signal. This problem is even larger for very inactive giants like HD 28305, which have no or only short-lived and small active regions. But even very active stars do not always give good results, since the observer has to wait until an uneven distribution of active regions occurs. During 2014 to 2019, TIGRE data of HD 28307 (θ^1 Tau) turned out to be of little use because of a lack of a necessarily uneven activity region distribution.

In their study of M dwarfs, Fuhrmeister et al. (2019) compare different period search algorithms and conclude that Gaussian Process (GP) modeling leads to the smallest number of false detections. A clear advantage of GP modeling is the fact that because of the stochastic nature phase shifts can be easily accommodated, while Fourier-based methods become more cumbersome. Hence, we here settled

for this approach. Nevertheless, considering the aforesaid, we see the here presented rotation periods as preliminary.

In several Hyades giants' S-index time series, variations are clearly visible already to the educated eye, see Fig. 2 and Fig. 3. Their GP analysis can be thought of as sets of random variables, of which any finite set has a joint normal distribution (see the book by Rasmussen & Williams (2006) for a detailed discussion of GPs). Hence, a GP is completely specified by a mean and a co-variance function, and the latter can be used to search for periodic variations. The chosen kernel function, which describes the covariance of the data, forms the basis of all GP modeling.

Here we use the kernel of the so-called *celerite* approximation Foreman-Mackey et al. (2017), which takes the form

$$k_{ij} = \frac{a}{2 + b} e^{-c\tau_{ij}} (cos(\frac{2\pi\tau_{ij}}{P}) + 1 + b) + \delta_{ij}\sigma^2, \quad (2)$$

where k_{ij} is the co-variance matrix, τ_{ij} is the modulus of the time difference of the time stamps t_i and t_j, a and b are normalization constants, c describes the lifetime of the features, P is the desired period and σ a term generating white noise; we refer to Fuhrmeister et al. (2019) for a more detailed description and discussion of the applied procedure. The kernel in the form of Eq. 2 has the property that the kernel matrix K can be inverted with $O(nlog(n))$ operations rather than by $O(n^2)$. This provides a massive advantage for large data sets, since the co-variance matrix of the data needs to be inverted many times during the modeling process.

The results of our GP modeling of the Mt. Wilson data are shown in Figs 4 for HD 28307, in Fig. 5 for HD 27697, and nin Fig. 6 for HD 27371. Since the chosen *python* implementation of *celerite* can handle only a single periodicity, we rectified the data by taking out the long-term cyclic variations, thereby concentrating on shorter term variability in which we expect to find the rotational signal.

In each of the GP diagrams (i.e., Figs. 4,5,6) we show the rectified time-dependence (black data points), the best-fit (in a maximum likelihood sense) model (purple solid line) as well as the model "error", i.e., the light purple shaded regions; clearly this "error" becomes largest during those times when no data is available. To better assess the modeling parameters we performed a Markov Chain Monte Carlo Analysis (MCMC) using the Python implementation of *emcee* Foreman-Mackey et al. (2013), and present (in Figs. 4,5,6) the resulting period-likelihood scatter plots from runs with 24000 MCMC realizations These figures show well defined peaks and hence preferred periods of the Mount Wilson data, which we estimate (from the "classical" Δ likelihood ≤ 1 approach as) to be $P_{HD\ 27697} \approx 148 \pm 9$ days, $P_{HD\ 27371} \approx 149 \pm 5$ days, and $P_{HD\ 28307} \approx 142 \pm 8$ days, see Table 2.

The so far six years of TIGRE data still cannot compete with the time-coverage of the Mount Wilson data, but the very good s/n of our HEROS spectrograph cameras should produce S-index series and calibration, which better resolve smaller physical variations and introduce less noise to the analysis. So far, TIGRE S-data yield a credible result already for one star:

For the active K giant, HD 27371 (γ Tau), TIGRE S-data produce a significant period of 137 days, which agrees, within the uncertainties, with the above value obtained from the Mount Wilson data (149 days, see Table 2). This is remarkable, given the independence, by instrumentation and epoch, of the respective data sets. Hence, for this star we are confident of a rotation period of about 143 days, when combining both datasets.

We also note that Auriére et al. (2015), based on Choi et al. (1995), already quote a rotation period of 140 days for the other active K giant HD 28307, using the very same Mount Wilson data, and in excellent agreement with our own analysis (142 days).

Furthermore, given the well-defined and very suggestive variations in the S-data series of both active Hyades giants, confidence in both these 142 day rotation periods is well justified.

However, the case of the inactive K giant HD 27697 is very different, its variations are very small. To us, therefore, it is not clear, whether its variation timescale of 148 days is a physical variation at all, and if so, really indicates the rotation period of that star. See below for a further argument, why we doubt that the hardly active giant HD 27697 should rotate as fast as its two active peers.

3.5 Estimate of the convective turnover-time

Inspecting the chromospheric and coronal activity of the Hyades giants as given in 2, we here showed a remarkably clear decrease in the average S-value and X-ray luminosity over the duration of central helium-burning of the Hyades K giants, much like we know it since long from cool main-sequence stars.

Unfortunately, there is no direct evidence of rotational spin-down for giant stars: For one of the two inactive giants (HD 28305) we have no rotation period at all, and the period obtained for the other one, HD 27697, appears to be of a lesser significance and is similar to the rotation periods of the active giants.

However, the very active giants HD 27371 and HD28307, which are just starting central helium burning, have trustable rotation periods of about 143 days. Hence, their rotation is five times slower than the solar rotation, despite their larger activity. Consequently, since their slower rotation cannot be an indicator of lower activity, it rather seems to relate to the very different structure of a K giant compared to the Sun.

In mean-field dynamo theory, the decisive parameters is the Rossby number, i.e., the ratio between rotational period and convective turn-over time of the given stellar structure. Depending on a suitable definition of the latter (see discussion and references in Mittag et al. (2018)) mean-field dynamo activity seems to work only for Rossby numbers smaller than unity. Whether or not this also holds for giants is unclear, but for the following discussion we assume this to be the case. Then, in the non-active limit, the rotational period becomes an empirical measure of the convective turn-over timescale and consequently, rotation periods of giants, and how they differ from convective-envelope main sequence stars, carry information on the giants' convective layers, where their dynamo is in operation.

Based on this idea, we estimate the empirical convective turn-over timescale of a K giant from scaling the solar case by the factor, by which the rotation period is longer than of a solar-type star of similar activity level, as studied empirically by Mittag et al. (2018). The two active Hyades K giants, with rotation periods of around 143 days, have an ac-

tivity level, which compares to solar-like stars with rotation periods on the order of 15 days (i.e. stars more active than the Sun), suggesting a scaling-factor in the rotation periods (K giants versus solar type stars) of about 10.

As shown by Mittag et al. (2018), the upper envelope to the observed stellar rotation period distribution coincides with stars of vanishing activity and a Rossby-number of unity, and so gives a good empirical estimate of the convective turn-over time. For stars like the Sun that work puts this empirical value at about 35.5 days (see 4^{th} line in their Table 1), consistent with rotating stellar evolution models of Kim & Demarque (1996), which follow in detail both meridional mixing and convection and obtain a "global" (or non-local) convective turn-over time for their solar model of 37.5 days. That value is the total travel-time of an imaginary bubble for rising through the whole convection zone.

Other studies use a "local" convection turn-over time for, mainly, half a pressure scale height H_P above the bottom of the convective layer. In the case of the Sun, classical dynamo models expect there the creation of the longitudinal magnetic field. The local convective turn-over time represents the average (local) travel-time of a bubble rising up by one convection length $l_c = \alpha_c \cdot H_P$. Hence, such different definitions and details of how the convection is described, result in different absolute scales of the respective computed convection turn-over times. Individual values obtained from different codes and empirical timescales may therefore differ from each other by at least a factor of two.

If we now apply the same rotation period scaling-factor from above, of about 10, to the minimal rotation period of the inactive Hyades K giants, we find values of about 350 days for HD 28305 and HD 27697. As discussed in the previous section, it seems impossible to verify this estimate empirically, unless we are lucky enough to observe an exceptional, long-lasting active region on one of these rather inactive giant stars.

Since this suggested 350 days minimal rotation period should characterize the convective turn-over timescale of the Hyades K giants, we can consult our stellar models to discuss the factor between the solar and the giant value – at least on a relative scale, as pointed out above. For this approach, the local convective turn-over time is a very practical quantity, as it is easy to retrieve from any stellar model, which is using the classical mixing-length theory. In this approach the average convection velocity at a radial point r is given by the expression

$$v_c(r) = \sqrt{\alpha H_P g(r) \Delta T(r)/2T(r)} = \sqrt{P(r)\Delta T(r)/\rho(r)T(r)}$$

where our code specifies at each of its 200 height points and at each time step the adiabatic bubble's temperature gain $\Delta T(r)$, the global gas properties $T(r)$, $P(r)$, and ρ, using $\alpha = 2.0$. The local convective turn-over time is then given by $\tau_c = \alpha H_P / v_c$, considering that $H_P = P/g\rho$ and that all these values are here taken for a radial point at half a pressure scale height above the bottom of the convection zone; note that only half a pressure scale height higher up, the velocities already increase by a factor of 2, which makes the absolute scale of local convective turn-over times very dependent on where they are taken.

On a relative scale, though, the picture emerging from our stellar models is quite instructive. Our solar model yields a local convective turn-over time of 17 days. Considering that a global turn-over time must be longer by some considerable factor, this is in good agreement with Kim & Demarque (1996), despite using here a much less sophisticated code. However, with our robust and fast code, we can compute stellar models far beyond the main sequence. A model matching the Hyades giants then suggests 450 days of local convection turn-over time.

Note, that the surface gravity of the K giant model decreases from the solar value by two orders of magnitude. Consequently, at the bottom of its large convection zone, the main differences occur in the pressure scale height, which rises by a factor of 20 in the K giant model, when compared to the solar model. Hence, the much larger pressure scale heights of the giant's convective envelope are the main driver for an almost 30 times larger convective turn-over time as compared to solar-type stars. However, the empirically expected factor (by how the rotation periods scale) is of only a factor 10, scaling nearly with g^{-1}.

The discrepancy between empirical timescales and what our models suggest does not much differ from earlier computational work by Auriére et al. (2015) (see their Fig. 5, and Charbonnel et al. (2017) for a more detailed description): Their local convective turn-over times near the bottom of the convection zone become very large for luminous red giants, as they seem to scale approximately with g^{-2}.

However, there is a fundamental problem with operating a solar-type dynamo in a giant, and this is probably the key to a better understanding: It seems impossible to have magnetic field loops rise all the way through the huge convective envelope of a giant without having them decay before reaching the photosphere, (Holzwarth & Schüssler 2001). And indeed, the discrepancies between empirical and model convective turn-over times in fact disappear, when we consider higher layers of the convective envelope of a giant star, where convective turnover-times are generally longer: In our K giant models, the convection velocity increases (and the local convective turn-over time decreases), driven by larger temperature gains of the adiabatically rising bubbles, by up to an order of magnitude towards intermediate convection layers. This is more than enough to reconcile the lower empirical factor of how much slower (only 10 times, not 30 times) the giant convection appears to be in the field-forming layer, when compared with the Sun.

Hence, giant convective envelopes may actually run a stratified dynamo (see Brandenburg (2005)), if the milder gravity-scaling of empirical convective turn-over times as suggested here is confirmed as a general behaviour – meaning that perhaps, with falling surface gravity, gradually higher convective layers become involved in growing the longitudinal field in ever larger convective envelopes.

4 DISCUSSION AND CONCLUSIONS

The main result presented in this study is that the two K giants of 2.75 $M_\odot$ ending central helium burning show much less chromospheric and coronal activity than the two of 2.62 $M_\odot$ beginning this 130 Myrs lasting phase. Even though we are dealing with only four stars, these observations are entirely consistent with the idea that magnetic activity, much like during central hydrogen burning of cool ($M < 1.5 M_\odot$,

convective envelope) main sequence stars, is decreasing during central helium burning of K giants, by the action of magnetic braking in both these cases.

We therefore conclude that, first, despite the relaxation of the core with the onset of central helium burning, K giant clump chromospheres are heated by noticeable magnetic activity, which is consistent with the detection of coronal X-rays of such stars in the solar neighborhood, see e.g. Hünsch et al. (1996a), and second, that magnetic braking dominates the evolution of magnetic activity during the stable phase of central helium burning.

We suggest magnetic braking to be at work during this phase. By the relatively faster decrease of activity during central helium-burning, when compared to central hydrogen-burning, it would be more than an order of magnitude faster than for cool main-sequence stars. That should in fact be expected, given that a Hyades K giant is, by radius, over 15 times larger than a cool main sequence star and so provides a much larger lever for magnetic coupling with its circumstellar and interstellar medium.

These conclusions complement an emerging wider picture of angular momentum evolution across the HRD: Asteroseismology work by Beck et al. (2012) and, e.g. Buysschaert et al. (2016), based on *Kepler* precision photometric monitoring, has proven that the still contracting cores of giants on the foot of the RGB are rotating up to ten times faster than the surface layers. Apparently, fast core contraction of stars with $M > 1.5 M_{\odot}$ in the Hertzsprung gap drives a core spin-up, since X-ray detections show them to have a strong activity (see Hünsch et al. (1996a), Hünsch et al. (1996b) and references given therein).

While it is not clear, how such a core spin-up could drive a dynamo and of which type, by analogue, a similar process seems to work in massive stars during their fast core contraction and ascent to the AGB, see the discussion by Schröder et al. (2018): The detections of magnetic field and chromospheric activity high up on the AGB demonstrate that, where in the HRD core contraction is fast (as for fast evolving massive stars), activity increases.

When, by contrast, the stellar core is fairly stable, as with K giants in central helium-burning, then magnetic braking seems to dominate the outcome. Furthermore, the resulting similarities between the activity of K giants and cool solar-type stars raise the surprising question, whether we see the same type of dynamo at work, despite their large structural differences.

Unfortunately, surface gravities of AGB stars are so low that the relevant pulsations to detect fast-spinning cores of such stars are too slow, and resonances too broad, to be observable. Consequently, asteroseismology is unable to provide direct evidence for what happens inside AGB stars. We need to study them by means of their rotational periods.

Consequently, further monitoring of chromospheric activity is required to strengthen the still sparse observational evidence for the Hyades K giants and other giants rotation periods. We hope to present such work in the near future, to derive approximate Rossby numbers from each activity degree and rotation period, in order to estimate empirical convective turnover-times for different giants and gravities. That information should provide important clues as to where in the giant convective layers its dynamo is actually working, and our studies of the four Hyades K giants already provide a first important milestone.

ACKNOWLEDGMENTS

This study made use of the services of the Strasbourg astronomical data centre. The authors are grateful for financial support by the joint bilateral project CONACyT-DFG No. 278156 and funding from the Deutsche Forschungsgemeinschaft in several related projects. We also wish to acknowledge the use of S-index data from the Mount Wilson Observatory HK Project, which was supported by both public and private funds through the Carnegie Observatories, the Mount Wilson Institute, and the Harvard-Smithsonian Center for Astrophysics starting in 1966 and continuing for over 36 years. These data are the result of the dedicated work of O. Wilson, A. Vaughan, G. Preston, D. Duncan, S. Baliunas, and many others. We further wish to acknowledge the spectra analysis tool iSpec by Blanco-Cuaresma et al. and we want to thank the anonymous referee for very helpful and concrete suggestions to improve this paper.

REFERENCES

Asplund, M., Grevesse, N., Sauval, A. J., & Scott, P. 2009, ARA&A, 47, 481
Aurière, M., Konstantinova-Antova, R., Charbonnel, C., et al. 2015, A&A, 574, A90
Ayres T.R., Brown A., Harper G.M., Bennett P.D., Linsky J.L., Carpenter K.G., Robinson R.D., 1997, ApJ 491, 876
Baliunas S.L., Hartmann L., Dupree A.K. 1983, ApJ, 271, 672
Baliunas S.L., Donahue, R.A., Soon, W.H., Horne J.H., Frazer J., Woodard-Eklund L., Bradford M., and 20 coauthors 1995, ApJ, 438, 269
Beck P.G., Montalban J., Kallinger T., et al. 2012, Nature, 481, 55
Blanco-Cuaresma S., Soubiran C., Heiter U., Jofré P. 2014, A&A, 569, A111
Blanco-Cuaresma S. 2019, MNRAS 486, 2075
Boller T., Freyberg M.J., Trümper J., et al. 2016, ApJ, 588, A103
Brandenburg A. 2005, ApJ, 625, 539
Buysschaert B., Beck P.G., Corsaro E., et al. 2016, A&A, 588, A82
Charbonnel C., Decressin T., Lagarde N., Gallet F., Palacio A., Auriére M., Konstantinova-Antova R., Mathis S.;, Anderson R.I., Dintrans B. 2017, A&A, 605, A102
Choi, H.-J., Soon, W., Donahue, R. A., Baliunas, S. L., & Henry, G. W. 1995, PASP, 107, 744
Duncan D.K., Vaughan A.H., Wilson O.C., Preston G.W., Frazer J.L.H., Misch A., Mueller J., Soyumer D., Woodard L., and 8 coauthors, 1991, ApJS 76, 383
Eberhard G., Schwarzschild K. 1913, ApJ, 38, 292
Flower P.J. 1996, ApJ 469, 355
Foreman-Mackey, D., Hogg, D.W., Lang, D., Goodman, J. 2013, PASP 125, 306
Foreman-Mackey, D., Agol, E., Ambikasaran, S., & Angus, R. 2017, AJ, 154, 220
Fuhrmeister, B., Czesla, S., Schmitt, J. H. M. M., et al. 2019, A&A, 623, A24
Gossage, S., Conroy, C., Dotter, A., Choi, J., Rosenfield, P., Cargile, P., Dolphin, A. 2018, ApJ 863, A67
A. Hempelmann, M. Mittag, J. N. González-Pérez, J.H.M.M. Schmitt, K.-P. Schröder, G. Rauw, 2016, A&A 586, A14
Holzwarth V., Schüssler M. 2001, A&A, 377, 251

Hubrig S., Plachinda S., Hünsch M., Schröder K.-P. 1994, A&A, 291, 890
Hünsch M., Schröder K.-P. 1996, A&A, 309, L51
Hünsch M., Schmitt J.H.M.M., Schröder K.-P, Reimers D., 1996, A&A 310, 801
Kim Y.-C., Demarque P. 1996, ApJ 457, 340
Konstantinova-Antova R., M. Aurére, C. Charbonnel, G. Wade, D. Kolev, A. Antov, S. Tsvetkova, K.-P. Schröder, N.A. Drake, P. Petit, and 13 coauthors, 2013, Bulgarian Astronomical Journal, Vol. 19, 14
Kurucz, R. 1993, ATLAS9 Stellar Atmosphere Programs and 2 km/s grid. Kurucz CD-ROM No. 13. Cambridge, Mass.: Smithsonian Astrophysical Observatory, 1993., 13
Linsky J.L., Haisch B.M., 1979, ApJ 229, L27
Lodieu, N., Smart, R. L., Pérez-Garrido, A., & Silvotti, R. 2019, A&A, 623, A35
Meynet G., Mermilliod J.-C., Maeder A. 1993, A&AS 98, 477
Mittag, M., Hempelmann, A., Gonzalez-Perez, J. N., & Schmitt, J. H. M. M. 2015, 18th Cambridge Workshop on Cool Stars, Stellar Systems, and the Sun, 18, 549
Mittag M., Hempelmann A., Schmitt J.H.M.M., Fuhrmeister B., González-Pérez J.N., Schröder K.-P. 2017, A&A 607, A87 (39pp)
Mittag M., Hempelmann A., Schmitt J.H.M.M., Schröder K.-P. 2018, A&A 618, A48
Perryman M.A.C., Brown A.G.A., Lebreton Y., Gomez A., Turon C., and 5 coauthors 1998, A&A 331, 81
Pietrinferni A., Cassisi S., Salaris M., Castelli F. 2004, ApJ 612, 168
Pietrinferni A., Cassisi S., Salaris M., Castelli F. 2006, ApJ 642, 797
Piskunov, N. E., Kupka, F., Ryabchikova, T. A., Weiss, W. W., & Jeffery, C. S. 1995, A&AS, 112, 525
Pols O.R., Tout C.A., Schröder K.-P., Eggleton P.P., Manners J. 1997, MNRAS, 289, 869
Pols O.R., Schröder K.-P., Hurley J.R., Tout C.A., Eggleton P.P. 1998, MNRAS, 298, 525
Rasmussen, C. E., & Williams, C. K. I. 2006, Gaussian Processes for Machine Learning, by C.E. Rasmussen and C.K.I. Williams. ISBN-13 978-0-262-18253-9,
Ramia P., Reddy B.E., Lambert D.L. 2019, MNRAS 484, 125
Salaris, M., & Bedin, L. R. 2018, MNRAS, 480, 3170
Schmidt-Kaler, T. 1982, in Landolt-B??rnstein: Numerical Data and Functional Relationships in Science and Technology - New Series, Group 6 Astronomy and Astrophysics, Vol. 2, 137
Schmitt J.H.M.M., Fleming TA., & Giampapa M.S. 1995, ApJ, 450, 392
Schmitt J.H.M.M., 1997, A&A, 318, 215
Schmitt J.H.M.M., Schröder K.-P., Rauw G. and 8 coauthors, 2014, Astronomische Nachrichten, 335, 787
Schröder K.-P., Pols O.R., Eggleton P.P. 1997, MNRAS, 285, 696
Schröder K.-P., Mittag M., Pérez Mart/'inez M.I., Cuntz M., Schmitt J.H.M.M. 2012, A&A, 540, A130
Schröder K.-P., Mittag M., Hempelmann A., González-Pérez J.N., Schmitt J.H.M.M. 2013, A&A, 554, A50
Schröder K.-P., Schmitt J.H.M.M., Mittag M., Gomez Trejo V., Jack D. 2018, MNRAS, 480, 2137
Skuminich A. 1972, ApJ 171, 565
Stern R.A., Zolcinski M.C., Antiochos S.K., & Underwood J.H. 1981, ApJ, 249, 647
Stern R.A., Schmitt J.H.M.M., & Kahabka P.T. 1995, ApJ, 448, 683
Vaughan A. H., Preston G. W., Wilson O. C. 1978, PASP, 90, 267
Wilson O.C., Bappu M.K.V. 1957, ApJ, 125, 661